Available online at www.sciencedirect.com
SCIENCE DIRECT®
Proceedings of the Combustion Institute 30 (2005) 1645–1653
Proceedings of the Combustion Institute
www.elsevier.com/locate/proci

Investigation of laminar pressurized flames for soot model validation using SV-CARS and LII

Klaus Peter Geigle[a,*], Yorck Schneider-Kühnle[a], Michael S. Tsurikov[a], Redjem Hadef[b], Rainer Lückerath[a], Véronique Krüger[a], Winfried Stricker[a], Manfred Aigner[a]

[a] *Institute of Combustion Technology, German Aerospace Center (DLR), 70569 Stuttgart, Germany*
[b] *Institut de Génie Mécanique, Université Larbi Ben M'hidi, 04000 Oum El Bouaghi, Algeria*

Abstract

Quasi-simultaneous measurements of temperature and soot volume fraction in pressurized and atmospheric flames are presented. A dual-flame burner concept yielded stable laminar flames for a variety of equivalence ratios, pressures, and fuels, and permitted the investigation of flames without the influence of soot oxidation. A CARS-based technique (shifted vibrational CARS) for temperature measurements, which offers high accuracy over the entire relevant temperature and soot concentration range, is described. Comparison of temperature measurements in the nonsooting part of a laminar diffusion flame at atmospheric pressure by SV-CARS and conventional N_2 Q-branch CARS yielded excellent agreement. This new technique was applied to quasi-1D laminar flames with soot concentrations up to 10 ppm and pressures up to 5 bar. The temperature profiles measured in these flames were combined with soot concentration measurements using LII; calibration and correction for signal trapping yielded quantitative soot volume fraction data. The temperature and soot concentration data were combined to generate a comprehensive dataset for the validation of an improved kinetic soot model for the prediction of soot formation in premixed combustion at elevated pressure.

Keywords: Laser diagnostics; Pressurized flames; Laminar premixed; Soot

1. Introduction

Soot has attracted increasing interest of politics, industry, and research due to its role as an undesirable byproduct of combustion processes and the thereby produced exhaust gases. A comprehensive understanding of processes involved in soot formation and oxidation is essential for the practical realization of pollutant reduction. In this context, considerable effort is directed at numerical modeling of soot formation. These models must, however, be extensively validated with experimental data. That must capture the phenomena of interest with sufficient resolution and must encompass a wide range of operating conditions. Two parameters vital to soot model validation are soot volume fraction (f_v) and local flame temperature (T). The latter is fundamental to the processes present in soot chemistry, and is thus particularly significant in the context of pollutant formation in combustion.

* Corresponding author. Fax: +49 711 6862 578.
E-mail address: klauspeter.geigle@dlr.de (K.P. Geigle).

1540-7489/$ - see front matter © 2004 The Combustion Institute. Published by Elsevier Inc. All rights reserved.
doi:10.1016/j.proci.2004.08.158

Flame temperature measurements via thermocouples, though tempting due to their relative simplicity, are limited in their accuracy by the need to correct for heat radiation, conduction, and convection. Thermocouples also influence the local flow field [1] and can suffer from coverage by soot, which prevents direct probe contact with the surrounding gas. Several nonintrusive techniques for temperature measurements in sooting environments have been published [2,3]. One approach measures the line-of-sight particle emission for a homogeneous soot distribution of equal temperature [4], which is then compared to a blackbody light source of known temperature. This method cannot be applied to nonsooting regions of a flame and is restricted to homogeneous soot and temperature distributions. Laser-based techniques offer the advantage of high temporal and spatial resolution without being limited to the stated restrictions. Temperatures in sooting flames are in principle accessible by rotational coherent anti-Stokes Raman scattering (CARS) [2] and filtered Rayleigh scattering [3]. However, the former shows a decreased sensitivity at flame temperatures, the latter is essentially dependent on knowledge of the local gas composition and the pressure (p), factors which strongly influence the relevant line-broadening and thus the measurement accuracy (an in-depth discussion is found in [5]). Vibrational N_2 Q-branch CARS is an accurate technique for temperature measurements in practical combustion, but the conventional excitation scheme based on a 532 nm Nd:YAG laser [6, p. 309] fails in sooting flames because of strong interference from laser-induced C_2 Swan band emission. Modified excitation schemes based on the inclusion of an additional dye laser to shift the CARS signal to less disturbed spectral regions have recently been published [7,8].

The development of soot models is strongly dependent on accurate temperature information in conjunction with soot concentration data measured in flames with different fuels, equivalence ratios (ϕ), and pressures. The phenomenology of soot formation at elevated pressure is of great importance since virtually all practical combustion devices operate at $p \gg 1$ bar. However, few experiments focusing on soot model validation at elevated pressures are available [9,10]. This is in part due to stringent requirements imposed by factors as flame instability and the thinning of the flame reaction zone at elevated p.

The current study addresses the aforementioned difficulties by combining well-resolved temperature (by SV-CARS; discussed below) and quantitative soot concentration measurements (by LII) with a versatile two-flame burner which provides stable, laminar, premixed flames for a variety of equivalence ratios and fuels for p up to 5 bar. These flames serve as quasi-1D model flames to study the pure, turbulence-free chemistry of soot formation. The described SV-CARS excitation/detection scheme promises even less interference from Swan band emissions than in [7]. The LII measurements are quantified by an extinction measurement and include a signal trapping correction, discussed in [11] and essential for strongly sooting flames.

2. Experimental setup

2.1. Burner

Kinetic soot model validation experiments using flames at elevated pressure pose a significant challenge for burner design. One requirement is a completely laminar flow resulting in a stable flame without any flickering. In this case, a direct correlation of height above burner (HAB) with the combustion process time scale is possible. The flame needs to be homogeneous over the probe volume to avoid variations in the measured quantity (i.e., f_v or T). For a comparison with true 1D kinetical computations, the influence from the flame edges must be as small as possible (infinite burner surface approximation).

The current burner design was developed from known burner concepts ([4] and high pressure burners in [9,10,12,13]) based on the above requirements. Two concentric flames are surrounded by an air coflow. An essential feature of this burner is the use of a nonsooting CH_4/air ring flame that surrounds the axisymmetric sooting flame to be studied. The ring flame reduces oxidizing influences from the flame edges and provides a hot shielding film against the surrounding cold coflowing air. The two-flame concept is also useful for flame stabilization, as even lifted sooting flames were stabilized (allowing T measurements below the reaction zone). Both flames were stabilized above water-cooled sintered bronze plates (pore size 12 μm). Additional flow conditioning and mixing of fuel and air was achieved by using small glass beads below the bronze matrices. The burner assembly was mounted into a pressure vessel with large windows for optical access.

Table 1 shows the settings for the flames discussed in this work. These were found by adjusting ϕ for both flames and three cold exit velocities (CH_4/air, studied fuel/air, and coflowing air). The gas flows were controlled by five mass flow controllers calibrated in-house. For toluene flames, the combustion air was passed through a saturizer system with the toluene concentration determined ex-situ after sampling part of the mixture. All flow rates were chosen to minimize horizontal flickering and/or vertical fluctuations in the sooting flame and to yield a large homogeneous area around the flame axis (perfectly flicker-free or homogeneous flames could not be attained due to

Table 1
Flame settings for the presented 1D model flames

Fuel	Inner ϕ	Inner flame $d = 41.3$ mm		Ring flame $d = 61.3$ mm		Coflow air $d = 150$ mm	
		Q (fuel)	Q (air)	Q (CH_4)	Q (air)	Q (air)	p
C_2H_4	2.40	1.84	12.6	7.14	41.5	460.2	5
C_3H_6	2.23	0.34	3.12	1.51	11.4	202	1
C_7H_8	1.75	0.098	2.49	4.65	29.6	275.7	3

All flow rates are in standard liters per minute. Pressure is in bars.

minute fluctuations in the flow controller regulating valves; the stability of flames, particularly at elevated pressures, is exceedingly sensitive to these). For further flame stabilization, a grid was positioned at HAB of 40 mm ($p > 1$ bar) or 45 mm ($p = 1$ bar). It consisted of a few coannular metal rings, 4 mm in diameter, with enough open space so as not to behave like a stagnation plate [9].

2.2. Measurement techniques

2.2.1. LII

As a frequently applied technique for the in-situ nonintrusive determination of f_v and particle size, laser-induced incandescence (LII) has gained increasing attraction over the recent years [13–16]. The technique is based on strong laser-induced heating of soot particles, followed by equilibration over several processes such as vaporization, heat conduction, and radiation. Under carefully chosen conditions of excitation laser energy, detection wavelength, and timing, the radiation intensity is proportional to f_v and can be quantified by calibration using an independent technique such as cavity ring-down spectroscopy [17,18] or extinction [19]. This yields a calibration constant C, which converts the emitted LII signal to f_v.

For LII excitation, we used a Nd:YAG laser at 1064 nm. A set of sheet forming optics ($f = -80$ mm cylindrical lens, $f = 1000$ mm spherical lens, rectangular aperture) produced a homogeneous sheet of approximately 30 mm in height and 170 μm in width, top-hat, and Gaussian in the vertical and transverse directions, respectively. A polarizer and a half wave plate were used to keep the laser sheet energy close to 35 mJ (0.68 J/cm^2) behind the flame; this value was chosen from a measurement of the LII signal response (Fig. 1), to ensure the signal was independent of laser energy fluctuations (shot-to-shot fluctuations and local inhomogeneities from beam steering or attenuation). The signal was detected perpendicular to the sheet with an intensified CCD camera through a 450 ± 10 nm interference filter.

To measure extinction, the laser was operated at 532 nm at low energies to avoid processes other than extinction in the flame. Both beams for LII measurements and calibration by extinction used the same optical pathway; small changes in the lens positions were necessary to account for the change of focal length with wavelength. A quartz plate reflected about 4% of the incident extinction sheet energy into a quartz cell filled with laser dye. The rest of the sheet was partially absorbed by the flame and directed into a second dye cell. The fluorescence from the cells could be imaged by the camera by adding a mirror in front of the camera, a 700 nm interference filter rejected stray light. For both measurements, 100 single shot images were averaged.

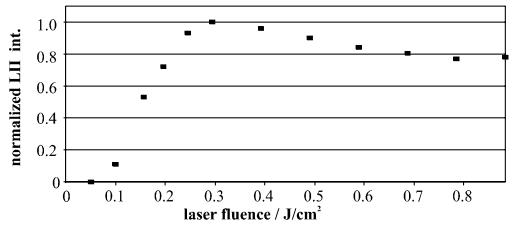

Fig. 1. Representative LII response as a function of the laser fluence measured at 1 bar.

It should be noted that for strongly sooting flames the energy losses (irrespective of process) in the LII and extinction laser sheets, determined by measuring the sheet energy with and without the flame, were observed to be different. The extinction (low energy) measurements indicate up to 80% absorption, while the LII sheet energy is attenuated by at most 30%. This clearly indicates that the LII process is not perfectly nonintrusive; in particular, the high LII laser fluences are known to result in increased soot sublimation, which can introduce additional error into the measurements. However, since LII signal generation starts simultaneously with particle vaporization, the initial (peak) signal is most representative of the true soot volume fraction and less sensitive to high laser fluences [14]. This "prompt detection" approach was therefore used in the current study with a 40 ns gate beginning with the laser pulse.

A critical issue in strongly sooting flames is that the detected LII signal is significantly lower than the emitted LII signal (required to calculate f_v via C) due to signal trapping along the path to the detector. While the difference can exceed 50%, the associated error in soot level on the burner axis did not exceed 15% because of a cancellation of effects: while the detected signal is reduced, the calibration procedure results in a larger C.

In axisymmetric flames, this effect can be corrected, modeling relevant physical processes more realistically and addressing a known error source. We followed the approach described in [11] that is based on the reconstruction of one complete emitted LII profile at a given HAB. The extinction measurement is described by:

$$\frac{I_{\text{ext}}}{I_{0,\text{ext}}} = \exp\left\{\frac{-kCL}{\lambda_{\text{ext}}}\sum_{n} S'_n\right\}, \tag{1}$$

where $I_{0,\text{ext}}$ and I_{ext} are the incident and attenuated extinction laser intensities at wavelength λ_{ext}, respectively, k is a function of the complex refractive index [11], and S'_n is the emitted LII intensity at detector pixel n. The extinction in a carefully chosen height (assumed to be equal to absorption) and the detected LII signal S_n (instead of S'_n) yield an initial guess for C and thus f_v. Based on that, the signal trapping is computed to deduce S'_n from S_n according to

$$S'_n = S_n \exp\left\{C\frac{k_{\text{det}}}{\lambda_{\text{det}}}\sum_{m=n}^{1} S'_m L_{n,m}\right\}, \tag{2}$$

where k_{det} is the corresponding dimensionless extinction constant for the detection wavelength λ_{det} and $L_{n,m}$ is the absorption path of the LII signal through a shell of soot (see Fig. 2). Eq. (2) is iterated adjusting C until the extinction (from soot) based on S'_n matches the measured value. The final value of C gives the true correlation of emitted LII signal to f_v. This constant applies for all other HAB, and the signal trapping for the signal emitted on the flame axis can easily be obtained from the height resolved extinction profile using the axisymmetry of the flame where the extinction beam and the emitted LII signal have to pass the same soot distribution (see Fig. 2):

$$I_{\text{ext}} = I_{0,\text{ext}} \exp\left\{-\sum_{r_0}^{r_n} f_v(r)\frac{k}{\lambda_{\text{ext}}}\Delta r\right\} \times \exp\left\{-\sum_{r_0}^{r_n} f_v(r)\frac{k}{\lambda_{\text{ext}}}\Delta r\right\}$$

$$S_{\text{sig}} = S_{0,\text{sig}} \exp\left\{-\sum_{r_0}^{r_n} f_v(r)\frac{k_{\text{det}}}{\lambda_{\text{det}}}\Delta r\right\}. \tag{3}$$

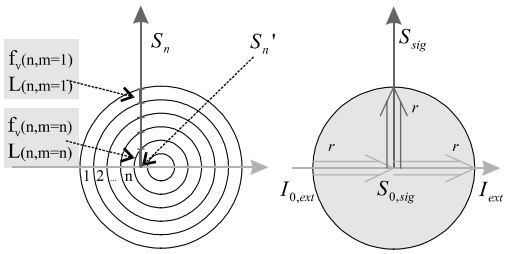

Fig. 2. Signal trapping correction for LII data analysis.

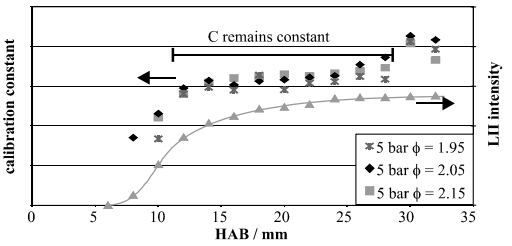

Fig. 3. Calibration of the LII signal (profile of $\phi = 2.15$ flame shown) with extinction measurements, showing a plateau region for C between HAB = 11 and 28 mm for different 5 bar propene/air flames.

We used the complex refractive index of 1.60–0.59i [20] for both the extinction wavelength (532 nm) and the LII signal wavelength (450 nm). Combination of Eq. (3) thus yields

$$\frac{S_{\text{sig}}}{S_{0,\text{sig}}} = \left(\frac{I_{\text{ext}}}{I_{0,\text{ext}}}\right)^{\frac{\lambda_{\text{ext}}}{2\cdot\lambda_{\text{det}}}}. \tag{4}$$

In contrast to other published data, where the integral extinction over the whole flame is measured [21], our setup allows us to choose the best calibration height for each measurement. The importance of this feature is illustrated in Fig. 3, which shows the typical variation of the "constant" C with HAB. At low HAB, extinction by soot is low. Thus, absorption by other species (e.g., PAHs) might influence the extinction measurement in a non-negligible way [22]. Furthermore, soot properties in the region of initial soot production are the least representative of the whole flame and not well known. At high HAB, soot particles start aging and form agglomerates, which again changes the optical properties. For data analysis, we used the region in between these extremes, i.e., close to the end of the soot volume fraction rise, where C remains constant and absorption is dominated by soot. Uncertainties in this and other LII parameters lead to an estimated f_v uncertainty of 30%.

2.2.2. SV-CARS

The CARS technique is based on measuring the temperature-dependent Boltzmann distribution of energy levels of a tracer species in the flame, and is a well-established and highly accurate tool for the determination of temperatures in various surroundings. The conventional setup of a N_2 vibrational CARS system uses the 532 nm output of a Nd:YAG laser for the pump wavelength. In sooting flames, the CARS laser beams excite laser-induced fluorescence from C_2 molecules, naturally present in flames but also produced by the interaction of the lasers with soot particles. This emission, shown in Fig. 4, occurs at the same λ as the N_2 CARS signal and can over-

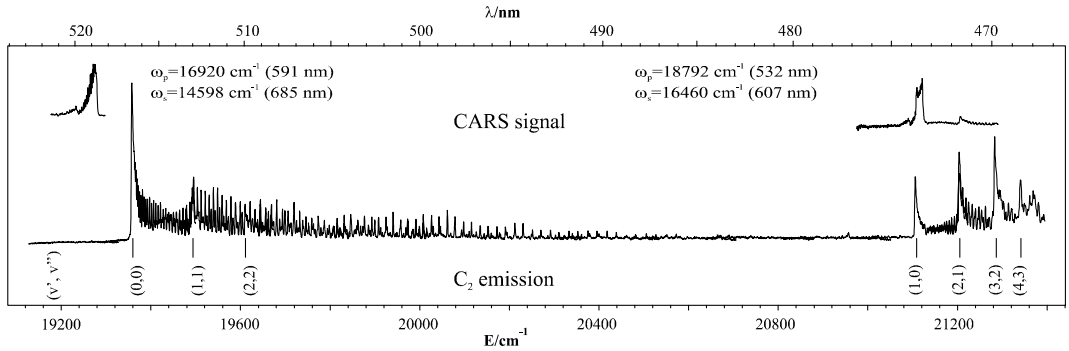

Fig. 4. C_2 Swan band in the relevant spectral range (bottom), together with typical spectra from conventional CARS (upper right) and SV-CARS (upper left), indicating full avoidance of interferences at 519 nm.

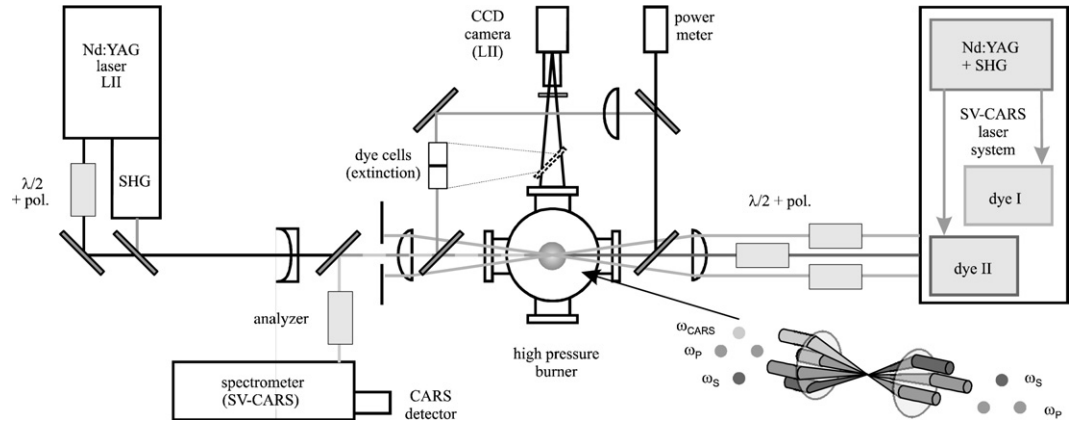

Fig. 5. Experimental setup, including the folded-BOXCARS phase-matching scheme, used for SV-CARS. The mirror in front of the LII camera is used to image the dye cells and is removed for the LII imaging.

whelm it. In lightly sooting flames, it is possible to analyze the CARS spectrum only in the undisturbed spectral regions (hot band), as done in [23]. This approach, however, reduces the measurement's accuracy and is not applicable for temperatures below 1300 K where the hot band in the *Q*-branch spectrum is too weak. Thus, conventional N_2 vibrational CARS in sooting flames is limited to the hot regime and to soot concentrations well below 0.1 ppm.

Our approach is to use a narrowband dye laser for the pump beams instead of the 532 nm Nd:YAG output, thus shifting the CARS signal out of the Swan bands (shifted vibrational CARS). In our experiment, the 532 nm output of a Nd:YAG laser was used to pump a narrowband dye laser (591 nm) which provided two pump beams and a home-built broadband dye laser (685 nm) that provided the Stokes beam. In contrast to earlier publications [7] or a dual-pump CARS approach [8], the CARS signal is now shifted to 519 nm instead of approximately 490 nm. As seen in Fig. 4, this region is completely undisturbed by C_2 emissions. This approach furthermore significantly reduces the overall laser-stimulated C_2 emission, since a Stokes beam at 685 nm can only excite the poorly populated $v \geqslant 3$ vibrational states of C_2 resonantly.

Figure 5 shows the entire experimental arrangement, including the SV-CARS system and the associated beam overlap scheme. The CARS beams were overlapped in their focus in folded BOXCARS geometry using a $f = 500$ mm lens; the resulting probe volume was approximately 4 mm long and 0.2 mm in diameter. This arrangement is advantageous due to its excellent spatial resolution (0.2 mm) normal to the burner surface, necessary for resolving steep flame temperature gradients, in particular in flames at elevated pressure; the larger (4 mm) dimension is not a problem since all flames were homogeneous over at least twice that width. All beams were equipped with polarizers and half wave plates for attenuation and for choice of proper beam

polarization to meet the phase-matching condition; an additional analyzer was implemented for background suppression in the case of pressurized flames (polarization CARS [6, p. 345]). The SV-CARS spectra were detected with a double spectrometer and an intensified CCD camera. At each flame position, 600 single pulse spectra were averaged. For normalization of the spectra, the spectral distribution of the broadband dye laser was measured from the nonresonant CARS signal excited in argon (average of 300 single spectra). The transfer function of the detection system was deduced from a N_2 spectrum at a known temperature (average of 300 single spectra). The spectra were analyzed for temperature by contour fitting calculated spectra to the measured ones [1].

The SV-CARS technique has an estimated error of 3% [24, p. 86] over the full temperature range, caused, e.g., by fit accuracy and uncertainty in chemical composition. Unlike methods related to blackbody radiators to determine the temperature, SV-CARS can deliver temperatures in all regions of a sooting flame, especially in the nonsooting flame front with steep gradients. The small probe volume gives an advantage over line-of-sight techniques that must assume (or prove) the homogeneity of the flame over the entire optical path. Furthermore, the technique allows single pulse measurements, resulting in additional information on local fluctuations via temporally resolved temperature measurements.

A typical "quasi-simultaneous" measurement sequence consisted of SV-CARS measurements, followed by LII and extinction measurements within a few minutes. This approach was applicable since the flames were temporally stable.

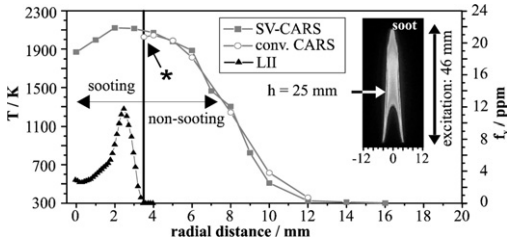

Fig. 6. Temperatures measured by conventional CARS and SV-CARS, showing good agreement in the nonsooting parts of the flame and demonstrating the ability of SV-CARS to measure temperatures reliably in the sooting regions. The CARS spectrum for the point labeled with * is shown in Fig. 4 upper right. Soot distribution is from [26].

3. Results and discussion

To validate the SV-CARS approach against conventional N_2 Q-branch CARS, a standard Gülder-flame burner for laminar diffusion flames [25] was used. Ethene and air were passed through coannular tubes of 12.5 and 88 mm in diameter at flow rates of 162 sml/min and 50 sl/min, respectively. A bed of glass beads provided flow conditioning for both flows. Under these conditions, the flame exhibited a visible length of 61 mm. Wiltafsky et al. [26] have shown flame reproducibility and applicability of this flame for calibration purposes. With a maximum soot volume fraction of approximately 12 ppm, this flame represents an ideal object for the validation of the modified CARS excitation scheme. As seen in Fig. 6, measurements show excellent agreement of SV-CARS with conventional CARS within the nonsooting regions; in addition, accurate temperatures in the sooting parts of the flame are now accessible. For example, the data point labeled with an asterisk in Fig. 6 was deduced from the conventional CARS spectrum shown in Fig. 4 (upper right) and was the last point accessible by conventional CARS; even there, the temperature fit clearly suffers from interferences, preventing an accurate data analysis. Remaining discrepancies at the flame edge showing a large temperature gradient are due to minor spatial day-to-day flame variations.

Representative results of the techniques when applied to pressurized flames are shown in Fig. 7, which presents data for the C_2H_4/air flame ($p = 5$ bar, $\phi = 2.40$). The shown LII uncertainty mainly arises from uncertainty in soot properties, the signal trapping procedure, and variations of the laser power through the flame. The maximum

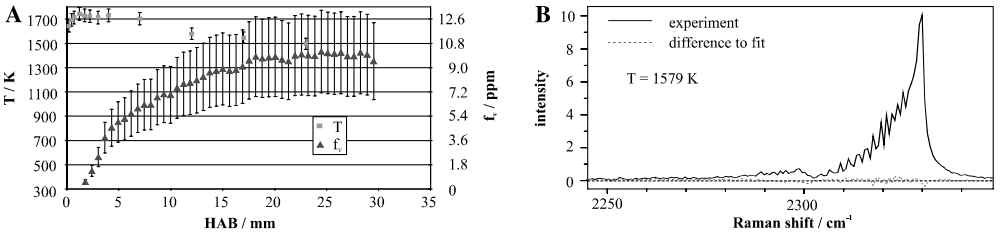

Fig. 7. T and f_v profiles in a strongly sooting C_2H_4/air model flame at 5 bar, $\phi = 2.40$ (A), CARS fit for HAB = 12 mm (B).

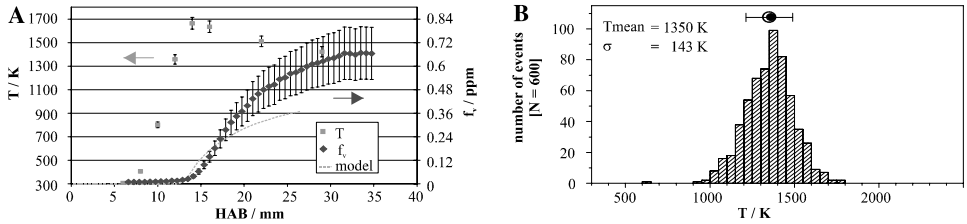

Fig. 8. T and f_v profiles in an atmospheric C_3H_6/air model flame at $\phi = 2.23$, together with results from kinetic soot model calculations [27] (dashed line, A) and temperature histogram at HAB = 12 mm (within temperature rise, B).

T and f_v values are 1740 K and 10.2 ppm, respectively; the latter value is similar to that in the aforementioned Gülder flame. The temperature at the lowest HAB accessible by SV-CARS (0.3 mm) is already near maximum. Detectable soot production starts approximately at the temperature maximum, i.e., close to the reaction zone. Figure 7B illustrates the fitting of the measured SV-CARS spectra for this flame at HAB = 12 mm, and demonstrates that, despite soot concentrations close to 8 ppm, interferences from C_2 Swan bands were not detected—again indicating the advantage of SV-CARS. Further data for other flame conditions are available on request.

The usefulness of these measurements in resolving both temperature and soot rise is illustrated in Fig. 8, which presents data for the C_3H_6 flame ($p = 1$ bar, $\phi = 2.23$). Atmospheric flames studied were frequently lifted above the burner, enabling measurements of temperature in the unreacted gases (a vital parameter for soot models). Again, soot formation starts close to the position of maximum temperature (1660 K). In this case, however, the temperature rises more slowly (roughly 1200 K over 6 mm). The often-used assumption of a local temperature step [28] is thus not justified here. Fig. 8 shows results that confirm this gradual temperature rise is in fact real and not the result of averaging over a thin, vertically fluctuating reaction zone. A histogram of T values at a point in the temperature rise would in this case exhibit a dual-mode behavior, showing alternately hot and cold temperatures. In contrast, the shown distribution is clearly single-mode. This slow temperature rise accurately resolved by SV-CARS must be accounted for by soot models.

Our earlier temperature measurements in sooting high pressure flames with conventional CARS [12] were limited to the regions below soot formation, but the implications of extrapolating these T values to the sooting regions are obvious [24, p. 64]. Similar to the earlier measurements, the present experiments show a significant temperature decay after the start of soot production, mainly caused by radiative losses. By using the temperatures derived from SV-CARS, modelers can account for these inherent losses that otherwise cannot be easily included in the model.

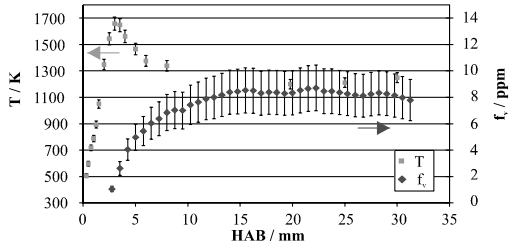

Fig. 9. T and f_v profiles in a strongly sooting toluene/air model flame at 3 bar, $\phi = 1.75$.

Figure 8 includes results of a kinetic soot model computation that used the measured T and f_v data as validation. This detailed model contains a relatively large gas phase reaction mechanism (520 reactions and 93 species) coupled with a mechanistic model for particle inception, coagulation, surface growth, and oxidation; details are provided in [27,29]. The model is seen to predict the position of soot rise and overall profile shape well; the measured and calculated f_v values agree remarkably well considering the state of the art of numerical soot models.

The profiles of the toluene/air flame (Fig. 9) show a slower temperature rise compared to the ethene flame. Here, T rises over 3 mm indicating a more complex fuel fragmentation chemistry. For the production of soot precursors and later soot particles, in this case the experimentally determined temperatures are even more important. As in the other presented flames, soot production starts close to the reaction zone. Even at a low ϕ of 1.75, the plateau soot level is quite high indicating the large soot formation potential of aromatic species. Since aromatics contribute significantly to liquid fuels, this dataset is relevant especially for kinetic studies with respect to fuels used in technical combustion.

4. Conclusions

Nonintrusive, well-resolved quasi-simultaneous temperature and soot volume fraction mea-

surements were successfully performed in premixed laminar flames at atmospheric and elevated pressures, with various fuels and equivalence ratios. The experiments were performed in the context of providing quantitative validation data for numerical soot formation models. Our coflame-burner design yielded stable, homogeneous laminar flames suitable for validation experiments. A new technique, SV-CARS, was successfully validated and applied to measure temperature in both sooting and nonsooting parts of the flame. These data were supplemented with accurate soot volume fraction data provided by LII measurements, which included careful calibration by extinction and correction for signal trapping within the flame. The data were shown to be useful to validate a kinetic soot model for one test case, yielding quite a good agreement between measured and calculated soot levels.

In addition to the benefit for kinetic model validation, at least in temporally stable flames, the gained accurate temperatures can be used to improve the typical uncertainty of estimated ambient temperatures for deduction of the particle size from LII decay curves. For example, Axelsson et al. [30] identified the ambient gas temperature as the main error source for particle sizing by time-resolved LII. Recent additional measurements were conducted in propene and toluene pressurized flames in our laboratory; the results are expected to improve the versatility of the kinetic soot model. Applicability of SV-CARS in turbulent environments is currently under consideration; this will strongly depend on sufficient beam overlap and will have to be proven.

Acknowledgments

The authors thank the Alexander von Humboldt Foundation for the award of a fellowship to R.H. and the Helmholtz-Gemeinschaft Deutscher Forschungszentren for funding during the program Particles and Cirrus Clouds (PAZI).

References

[1] R. Lückerath, M. Woyde, W. Meier, W. Stricker, U. Schnell, H.C. Magel, J. Görres, H. Spliethoff, H. Maier, *Appl. Opt.* 34 (1995) 3303–3312.
[2] L. Martinsson, P.E. Bengtsson, M. Aldén, S. Kröll, J. Bonamy, *J. Chem. Phys.* 99 (1993) 2466–2477.
[3] D. Hofmann, A. Leipertz, *Proc. Combust. Inst.* 26 (1996) 945–950.
[4] H. Jander, N. Petereit, D.M. Razus, *Z. Phys. Chem.* 188 (1995) 159–175.
[5] D. Most, A. Leipertz, *Appl. Opt.* 40 (2001) 5379.
[6] A.C. Eckbreth, *Laser diagnostics for combustion temperature and species*, second ed. Gordon and Breach Publishers, Amsterdam, 1996, p. 309, p. 345.
[7] Y. Schneider-Kühnle, R. Lückerath, W. Stricker, *European CARS Workshop*, Moskau, 2000; W. Stricker, in: K. Kohse-Höinghaus, J.B. Jeffries (Eds.), *Applied Combustion Diagnostics*, Taylor & Francis, New York, 2002, p. 181.
[8] F. Beyrau, A. Datta, T. Seeger, A. Leipertz, *J. Raman Spectroscopy* 33 (2002) 919–924.
[9] T. Pape, *Optische Untersuchungen zum Rußwachstum in vorgemischten Ethen-Luft Flammen bei 15 bar*, Diplom-Thesis, Göttingen, 1993.
[10] S. Hanisch, H. Jander, T. Pape, H.G. Wagner, *Proc. Combust. Inst.* 25 (1994) 577–584.
[11] D.J. Bryce, N. Ladommatos, H. Zhao, *Appl. Opt.* 39 (2000) 5012–5022.
[12] M. Braun-Unkhoff, A. Chrysostomou, P. Frank, E. Gutheil, R. Lückerath, W. Stricker, *Proc. Combust. Inst.* 27 (1998) 1565–1572.
[13] M. Hofmann, W.G. Bessler, C. Schulz, H. Jander, *Appl. Opt.* 42 (2003) 2052–2062.
[14] R.J. Santoro, C.R. Shaddix, in: K. Kohse-Höinghaus, J.B. Jeffries (Eds.), *Applied Combustion Diagnostics.* Taylor & Francis, New York, 2002, 2002, p. 252.
[15] R. Starke, B. Kock, P. Roth, *Shock Waves* 12 (2003) 351–360.
[16] H.A. Michelsen, P.O. Witze, D. Kayes, S. Hochgreb, *Appl. Opt.* 42 (2003) 5577–5590.
[17] R.L. Vander Wal, *Proc. Combust. Inst.* 27 (1998) 59–67.
[18] C. Moreau, E. Therssen, X. Mercier, J.F. Pauwels, P. Desgroux, *Appl. Phys.* B, accepted.
[19] J. Appel, B. Jungfleisch, M. Marquardt, R. Suntz, H. Bockhorn, *Proc. Combust. Inst.* 26 (1996) 2387–2395.
[20] T.T. Charalampopoulos, J.D. Felske, *Combust. Flame* 68 (1987) 283–294.
[21] B. Axelsson, R. Collin, P.E. Bengtsson, *Appl. Phys. B* 72 (2001) 367–372.
[22] M.Y. Choi, A. Hamins, G.W. Mulholland, T. Kashiwagi, *Combust. Flame* 99 (1994) 174–186.
[23] Ö.L. Gülder, D.R. Snelling, R.A. Sawchuk, *Proc. Combust. Inst.* 26 (1996) 2351–2357.
[24] Y. Schneider-Kühnle, *Experimentelle Untersuchung rußender Hochdruckflammen mit laserdiagnostischen Messmethoden*, Ph.D. thesis, Stuttgart, 2004, p. 86, p. 64.
[25] Ö.L. Gülder, *Combust. Flame* 92 (1993) 410–418.
[26] G. Wiltafsky, W. Stolz, J. Köhler, C. Espey, *SAE Tech. Paper 961200*, Society of Automotive Engineers, Warrendale, PA, 1996.
[27] K.P. Geigle, Y. Schneider-Kühnle, V. Krüger, M. Tsurikov, R. Lückerath, M. Braun-Unkhoff, N. Slavinskaya, P. Frank, W. Stricker, M. Aigner, in: *Proceedings of the European Combustion Meeting, European Section of the Combustion Institute*, Orléans, France, 2003.
[28] M.M. Maricq, S.J. Harris, J.J. Szente, *Combust. Flame* 132 (2003) 328–342.
[29] D. Hu, M. Braun-Unkhoff, P. Frank, in: U. Schumann, G.T. Amanatidis (Eds.), *Air Pollution Research Report 74—Aviation, Aerosols, Contrails and Cirrus Clouds (A^2C^3)*. Seeheim, 10–12 July, 2000, European Commission, Brussels, p. 85.
[30] B. Axelsson, R. Collin, P.-E. Bengtsson, *Appl. Opt.* 39 (2000) 3683–3690.

Comments

Per-Erik Bengtsson, Lund Institute of Technology, Sweden. Results of line-broadening effects from product gas species on N_2 lines in rotational CARS thermometry have been presented [1]. For example, inclusion of N_2-CO broadening will have a large influence on temperature (tens of K) in sooting flames. In your vibrational CARS work in sooting flames, did you consider other line-broadening species than CO_2 and H_2O? If not, can you estimate the errors introduced by not considering N_2-CO and N_2-H_2 broadening, given the fact that CO and H_2 have concentrations above 15% in premixed sooting ethylene flames?

Reference

[1] F. Vestin, M. Afzelius, C. Brackman, P.-E. Bengtsson, *Proc. Combust. Inst.* 30 (2005) 1673–1680.

•

Reply. We are aware of the fact that significant major species concentrations in sooting flames might influence the accuracy of temperature measurements with vibrational CARS. The line broadening by H_2O and CO_2 as colliding species [1,2] and theoretically derived collision broadening effects for H_2 [3] are already included in our fitting algorithm. We have not performed further investigations in that direction, especially those dealing with N2-CO collisions. However, we expect the influence to be lower compared to measurements with rotational N_2 CARS. For an approximation of the induced error based on a 10 % concentration, we replaced the originally used N_2 self-broadening for N_2-CO collisions by either H_2O or H_2 as collision partner. The influence of the true CO line-broadening should be found between both of these extrema. At one selected measurement point in both cases the resulting variation in temperature was on the order of 10 K at flame temperatures, but still not visible in the fit quality. This is within the general accuracy of CARS temperature measurements.

References

[1] G. Millot, *J. Chem. Phys.* 93 (1990) 8001–8010.
[2] M. Fischer, E. Magens, A. Winandy, XIV European CARS Workshop, Escorial (Spain), 1995.
[3] J. Hussong, R. Lückerath, W. Stricker, X. Bruet, P. Joubert, J. Bonamy, D. Robert, *Appl. Phys. B* 73 (2001) 165–172.

•

Greg Smallwood, National Research Council Canada, Canada. As a comment, temperature has been measured [1] in a sooting laminar diffusion flame using vibrational CARS, employing selective fitting regions to avoid C_2 Swan band interference. The precision was $\pm$ 25–50 K at 1700 K. It is unclear why it was necessary for the use of shifted vibrational CARS, as it does not appear to offer improved precision over the existing technique.

The LII technique is highly dependent upon the calibration constant. How much did this constant vary with pressure and with fuel type? Why is there any variation in the "constant"? Can you be sure that the constant is applicable at all locations in a given flame, considering its variation in flames of different pressure and fuel composition?

Reference

[1] Ö.L. Gülder, D.R. Snelling, R.A. Sawchuk, *Proc. Combust. Inst.* 26 (1996) 2351–2357.

•

Reply. Our detected spectral features, dependent on the experimental setup, look very much different. The actually presented CARS spectrum excited with the usual excitation scheme suffers from Swan band emission, not from absorption. The difference is probably due to a different experimental setup. Neither absorption nor emission interference is present in SV-CARS spectra. In our opinion, a completely undisturbed spectrum should result in the best available data for a precise fit and thus the most reliable temperatures, especially over the whole temperature range. For future single pulse application of the technique to turbulent flames, the advantage of a fit of the entire spectrum will be essential.

Comparison of 46 different experiments performed over 2 years resulted in a scatter of the determined calibration constant of approx. $\pm$ 18 %, and not following a significant trend with variation of fuel or pressure. These variations might be due to minor changes of the optics, e.g. soot on windows, exact position of calibration, laser beam profile and exact laser power. A calibration constant determined individually for each flame is, in our opinion, the best available value considering the current state of the art; furthermore, its accuracy is qualitatively definitely not worse than that of the refractive index of soot. Even if the constant were not representative, especially for the early regions of soot formation of a single flame, the soot profile would not change dramatically, since in these regions of soot formation the absolute error on the relatively low soot concentrations would be low.